Anisotropic grossular–andradite garnets: Evidence of two stage skarn evolution from Rudnik, Central Serbia

Bojan Kostić, Danica Srećković-Batoćanin, Petyo Filipov, Pavle Tančić, Kristijan Sokol

GEOLOGICA CARPATHICA, FEBRUARY 2021, 72, 1, 17–25 https://doi.org/10.31577/GeolCarp.72.1.2

Anisotropic grossular–andradite garnets: Evidence of two stage skarn evolution from Rudnik, Central Serbia

BOJAN KOSTIĆ[1,✉], DANICA SREĆKOVIĆ-BATOĆANIN[1], PETYO FILIPOV[2], PAVLE TANČIĆ[3] and KRISTIJAN SOKOL[1]

[1]Faculty of Mining and Geology, University of Belgrade, Djusina 7, 11000 Belgrade, Serbia; ✉bojan.kostic@rgf.bg.ac.rs
[2]Bulgarian Academy of Sciences, Acad. G. Bonchev-Str. Build. 24, 1113 Sofia, Bulgaria
[3]Geological Survey of Serbia, Rovinjska 12, 11000 Belgrade, Serbia

(Manuscript received November 1, 2020; accepted in revised form December 21, 2020; Associate Editor: Igor Broska)

Abstract: This paper presents LA-ICP-MS data for garnets from the Rudnik skarn deposit (Serbia), which range from $Grs_{45–58}Adr_{40–52}Alm_{2–3}$ in the core and $Adr_{70–97}Grs_{2–29}Sps_1$ in the rim displaying anisotropy and zoning. In spite of wide compositional variations the garnets near the end-member of andradite (Adr>90) are generally isotropic. Fe-rich rims exhibit LREE depletion and flat HREE pattern with weak negative Eu anomaly, including higher As and W contents. On the other side, the Fe-poorer core shows flat REE pattern without any significant enrichment or depletion of REE, except higher amounts of trace elements, such as U, Th and Zr. Presence of sulphide minerals indicates reduction conditions and Eu divalent state. Different REE behaviour is conditioned by Eu^{2+} in reduction conditions. The observed variations in optical features and garnet chemistry are the results of their two-stage evolution. The first stage and period of garnet growth is probably buffered by mineral dissolution and reactions in the country rock. The second stage is related to hydrothermal activity when W and Fe were brought into the system probably by a boiling process in the volcanic event in the late Oligocene 23.9 Ma.

Keywords: grandite, garnets, skarn, Rudnik.

Introduction

Study of the composition of common skarn minerals and the possibility to be helpful in prospecting of skarn deposits has a brief history. One of the earliest attempts was made by Nakano et al. (1991) who studied the composition of pyroxenes. Afterwards, several attempts were made for garnet. Despite their highly variable composition due to a number of substitutions that may take place in the structure, garnet becomes a suitable geochemical tracer. Such application is supported by its common presence in skarn deposits and its high physical and chemical stability during weathering. Additionally, this mineral is easy recognizable under the microscope, and quite often macroscopically, as well. The discovery that the andradite-rich garnets contain more Cu than grossular-rich opened a question: whether garnet chemistry could be used as a guide in prospecting Cu-skarn deposits (Somarin 2004)? Use of the rare earth elements (REE) in studies of the nature and effects of hydrothermal alterations and hydrothermal systems is a relatively new method as the REE were commonly regarded as insensitive to all, except to the hydrothermal processes (Gaspar et al. 2008).

Although the grossular–andradite (grandite) garnets are the commonest in skarn deposits, several studies concerning the composition of REE in garnets are available up to date (e.g. Jamtveit & Hervig 1994; Nicolescu et al. 1998; Smith et al. 2004; Gaspar et al. 2008; Zhai et al. 2014; Park et al. 2017; Xiao et al. 2018).

Zonation patterns of skarn garnets as indicator of changes in hydrothermal systems during garnet growth have been discussed by several researchers (e.g. Jamtveit et al. 1993, 1995; Pollok et al. 2001). Oscillatory zoning in skarn minerals, particularly in grandite garnets are common in shallow contact metamorphic aureole (Smith et al. 2004).

To the best of our knowledge, only two optically anisotropic and oscillatory zoned grandite samples from Serbia have been characterized in more or less detail: Tančić et al. (2012) studied macroscopically visible zoned $Grs_{58–64}Adr_{36–42}Sps_2$ sample from Meka Presedla (Kopaonik Mt.) with optical microscopy, electron microprobe analysis (EMPA), and FT–IR and Raman methods. It is entirely slightly anisotropic and without presence of isotropic areas, which was primarily caused by its non-cubic structural dissymmetrization (Tančić et al. 2020). Srećković-Batoćanin et al. (2014) studied two $Adr_{51–97}Grs_{3–47}Sps_{0–2}$ and $Adr_{79–100}Grs_{0–19}Sps_{0–1}$ samples from Rogozna Mt. In addition, the behaviour of REE in grandites from the same locality was studied by Mladenović et al. (2018).

This study presents the results of investigations of zoning grandite patterns in skarn samples SN-310 from the borehole coordinates (44.125887°N, 20.507926°E), applying optical microscopy, EMPA and LA-ICP-MS methods, with the aim of constraining hydrothermal system evolution. The observed trend of the REE in garnet is useful for understanding the mechanisms for incorporation of trace elements and REE into garnets and highlighted the evolution of the hydrothermal system. Zircon dating was done on Q-latitic dyke from a borehole

(sample SN-330). Second zircon dating was done on a shallow volcanic body on the north-west of Rudnik (sample SN-313, coordinates: 44.165312°N, 20.476853°E). These two types of volcanic bodies are dated using zircon to obtain U–Pb ages and link between volcanism and metamorphism, temporally as well as spatially in the Rudnik area.

Geological setting

The studied area is located in Serbia ~80 km south of Belgrade on the central axis of the Sava Zone that is interpreted as a suture of the final closure of the northern Neotethys branch (Schmid et al. 2008). The Mesozoic geology of the central Balkan Peninsula reflects the evolution of the Vardar branch of the Neotethys in several episodes, including Permian–Triassic opening, Late Jurassic ophiolite obduction, Cretaceous subduction and Cenozoic post-collisional orogenic development (see Schmid et al. 2008; Cvetković et al. 2016; Prelević et al. 2017). The Sava Zone (suture zone) separates the Carpatho–Balkan orogen (a part of the Dacia Mega-unit and Tisza), from the southerly and westerly Adria derived thrust sheets, namely the Dinarides (Pamić & Šparica 1983; Haas & Péró 2004). Trending NNE from Belgrade the Sava Zone is mostly represented by Late Cretaceous flysch.

In the adjacent region, Cenozoic orogenic post-collisional processes were caused by NW movement of Adria derived units. Geotectonic regimes were successively changed over time from generally compressive to strike-slip or completely extensional tectonic style (Cvetković et al. 2016). This extension was linked to Miocene back-arc formation in the Pannonian basin (Horváth et al. 2006; Ustaszewski et al. 2010). The extension induces gravitational instability of the Dinaride orogen with ruptures, which have reached the bottom of the lithosphere triggering the melting of the upper lithosphere, previously metasomatized by crustal material (Cvetković et al. 2004, 2014; Prelević et al. 2005). This trigger produced volcanic activity with elevated potassium content in the Miocene, in some parts of the Adria–Europe suture zone (Prelević et al. 2005).

The Cretaceous sediments in the vicinity of Rudnik Mt. (Fig 1.) were described as clastic "paraflysch" (Anđelković 1973; Dimitrijević & Dimitrijević 2009) as these sediments resemble typical flysch but lack characteristic internal organization. The Lower Cretaceous includes shales, mudstones, sandstones and limestones which sometimes look like immature turbidites (Dimitrijević & Dimitrijević 1987, 2009; Sladić-Trifunović et al. 1989). Going upwards in the stratigraphic scheme, Lower Cretaceous sediments are replaced with shallow water reef limestones and clastics. The Upper Cretaceous succession starts with Albian–Cenomanian conglomerates, microconglomerates, sandstones, carbonates, and continental shales (Brković 1980). Numerous volcanic bodies, referred to as quartzlatitic stocks and dykes, crosscut through Cretaceous carbonate–sandstone–shale sequences developing local contact metamorphic aureoles. So far, evidence of a plutonic body has not been confirmed. Borehole data show that Cretaceous sediments are in tectonic contact with peridotites (harzburgites) in the footwall, which are exposed in Stragari locality on the east side of Rudnik Mt. In the contact zone metamorphic rocks are often represented by hornfels and skarns which host polymetallic Pb–Zn mineralization. The ore bodies are predominantly composed of pyrrhotite, galenite, sphalerite, chalcopyrite and arsenopyrite (Stojanović et al.

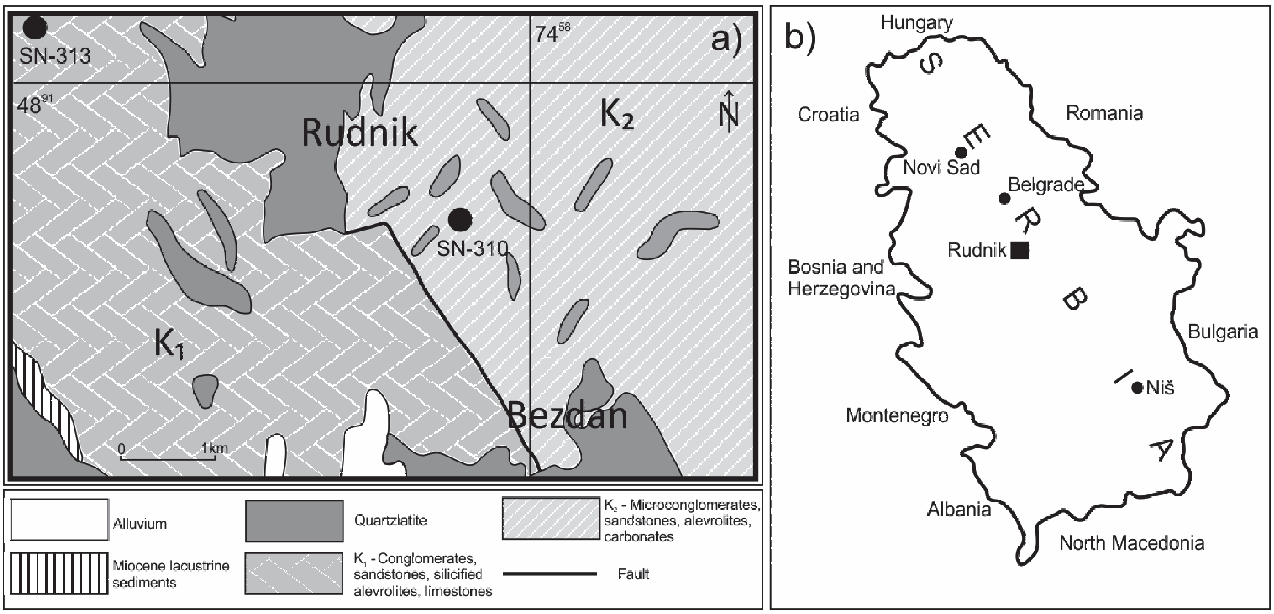

Fig. 1. a — Simplified geological map of Rudnik area modified according to the Basic geological Map 1:100,000, Sheets Kragujevac (Brković et al. 1980) and Gornji Milanovac (Filipović et al. 1978); **b** — Exact position of investigated area within Serbia.

2018). A small amount of magnetite, cassiterite and scheelite can be found only locally (Stojanović et al. 2018). Within the south part of the Rudnik skarn deposit, lateral zoning in contact aureole is weakly displayed and closely related to the protolith. It is represented by quartz, epidote, zoisite, chlorite, calcite, and minerals from the actinolite–tremolite group, while in more skarnized zones garnets and pyroxenes occur. Miocene sediments (conglomerates, sandstones, and clays) cover only a small area to the NW and SE of Rudnik. Miocene sedimentary rocks show metamorphic alteration only in the zones of direct contact with volcanic rocks.

Analytical methods

Major elements were obtained by EMPA using a JEOL 6610 LV electron microprobe equipped with wavelength-dispersive spectrometer (Oxford Instruments Wave 700) at the University of Belgrade, Faculty of Mining and Geology. Conditions for microanalysis were spot size 2 μm, an accelerating voltage of 30 kV and a beam current of 10 nA, using natural and synthetic mineral standards including albite (Al, Si), wollastonite (Ca), titanium monoxide (Ti), chromium oxide (Cr), and manganese (Mn) and iron (Fe) metal. Backscattered (BSE) images were used to reveal zoning and possibly inclusions of another mineral phase within the garnet and zircon crystals. Cathodoluminescence (CL) imaging was obtained for identifying inherited cores, cracks and inclusions inside zircon grain.

U–Pb in-situ zircon dating and trace elements analyses of garnet were performed at the LA-ICP-MS laboratory of Geological Institute in Sofia, using New Wave UP193FX LA coupled to Perkin Elmer ICP-MS. Laser parameters were tuned at ablation crater of 35 μm for dating, and 50 μm for tracing. The ablation frequency was 8 Hz. Measurements were calibrated with GJ1 zircon standard (Jackson et al. 2004) as external standard for fractionation correction, and 91500 standard zircons (Wiedenbeck et al. 1995) were used as unknown to correct systematic error. Reference material NIST610 was used as standard material for trace elements. Data reduction was processed through Iolite software v2.5 (Paton et al. 2011), applying down-hole fractionation correction to all the analyses. Zircon age diagram plots and concordia ages were obtained using Isoplot 3.75 application (Ludwig 2013).

Results

Petrography of Rudnik orefield skarn

Garnet skarns are subsidiary in the contact-metamorphic aureole around the Rudnik orefield. The analysed sample SN-310 was collected from the borehole at the 289 m depth. The units discovered by the borehole start with coarse-grained conglomerate containing fragments/clasts from quartzite, chert and altered peridotites. These rocks are, as a rule, followed by alternated microconglomerates and sandstones. The sandstones continue downward through limestones with more or less terrigenous component. The carbonate unit is not of constant thickness in respect to the clastic ones, which are closer to the surface. Marlstones, almost pure limestones and transitional varieties were recognized within the carbonate unit, depending on the amount of clastic component. Carbonate rocks alternate with fine-grained rocks considered hornfelses. All these units display contact metamorphic alteration from metaconglomerate and metasandstones to skarns. The exception is at their contacts with peridotites in the footwall where only slightly recrystallized calcite could be noticed. Skarns occur as small-scale bodies up to a few metres thick. Their texture is either granoblastic or nematoblastic, and structure is massive, rarely banded. The selected sample for detailed analyses contains calcite+garnet+epidote+chlorite+quartz (Fig. 2). Garnets throughout the overall skarn zone tend to form euhedral crystals and usually contain epidote and opaque minerals as inclusions. They are optically zoned, having anisotropic core and isotropic rim. Recrystallized calcite with rare epidote grains, was matrix in the protolith rock. Epidote grains are optically zoned and anhedral. Chlorite often appears in radial forms and displays Berlin blue interference colours. The last constituent, quartz, is a terrigenous component and is mixed with calcite.

U–Pb dating on zircons

Zircons were taken from two separate volcanic bodies. The first sample SN-313 comes from the borehole in the shallow massive quartz latite intrusion north-west from Rudnik Mt. Another sample, SN-330, was taken from a quartzlatitic sill/dyke about 25 m thick, which has also been accessed by borehole. These quartz latites cut Upper Cretaceous sediments that have been metamorphosed into skarns and hornfels in the vicinity of Rudnik village (Fig. 1). The results for both samples point to crystallization ages at 23.9 Ma on the U–Pb Concordia diagrams (Fig. 3). No inherited cores were found in zircons from the two samples.

Zonation and garnet chemistry

Rudnik garnet shows the zoning pattern which can be described primarily as inhomogeneous garnet core with zoned rim. This indicates significant changes in garnet chemistry, which can be observed in polarized light under microscope as well as in BSE images using scanning electron microscopy (Figs. 2, 4). The darker zones in BSE images are richer in Al while lighter zones are of a higher Fe content (Table 1). FeO obtained by EPMA was converted to $FeO+Fe_2O_3$ by assuming that deficiency of Ti+Al+Cr for the octahedral M site is made up by Fe^{3+}.

According to obtained results the studied garnets from the Rudnik orefield are predominantly grossular–andradite solid solutions being roughly $Grs_{45–58}Adr_{40–52}Alm_{2-3}$ (grain 1:

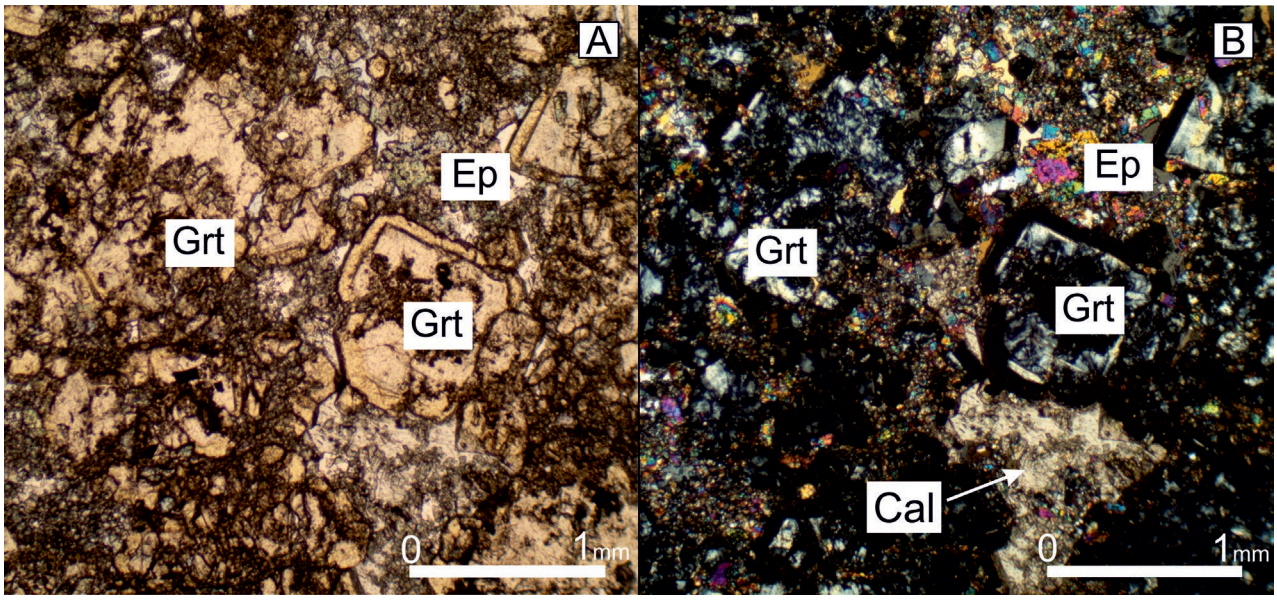

Fig. 2. Photomicrograph of anisotropic garnets in skarn sample SN-310 taken from the borehole: **A** — PPL; **B** — XPL

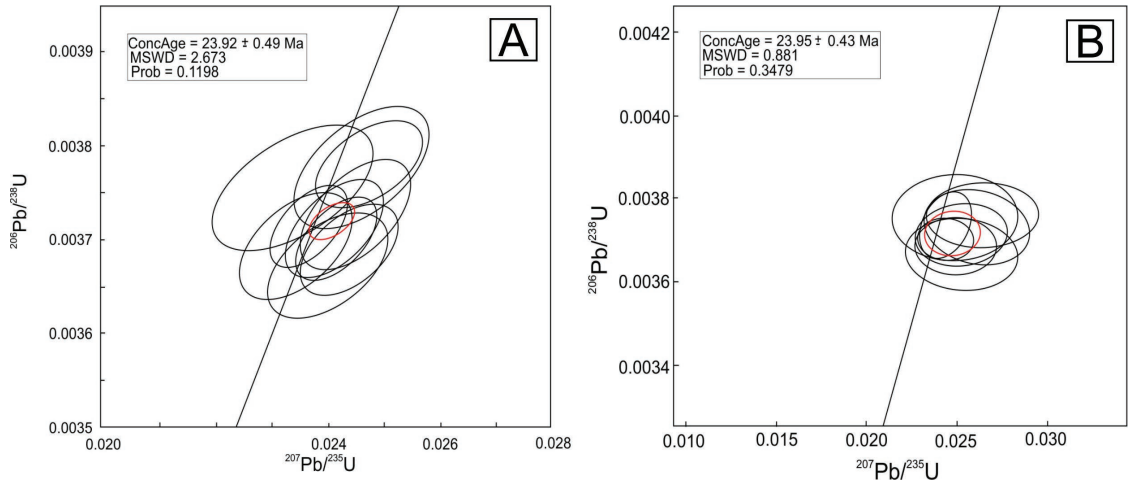

Fig. 3. Obtained age for shallow volcanic body (SN-313) and dyke (SN-330) are shown on U–Pb concordia diagrams.

$(Ca_{2.949}Fe^{2+}_{0.051}Mn_{0.000})_{3.000}(Al_{1.198}Fe^{3+}_{0.802}Cr_{0.000}Ti_{0.000})_{2.000}(Si_{2.991}Al_{0.009})_{3.000}$ and grain 2: $(Ca_{2.909}Fe^{2+}_{0.091}Mn_{0.000})_{3.000}(Al_{0.961}Fe^{3+}_{1.038}Cr_{0.001}Ti_{0.000})_{2.000}(Si_{3.012}Al_{0.000})_{3.012}$) in the core and $Adr_{70–97}Grs_{2–29})Sps_1$ (grain 1: $(Ca_{2.991}Fe^{2+}_{0.000}Mn_{0.018})_{3.009}(Al_{0.588}Fe^{3+}_{1.363}Cr_{0.000}Ti_{0.041})_{1.991}(Si_{2.962}Al_{0.038})_{3.000}$ and grain 2: $(Ca_{2.968}Fe^{2+}_{0.011}Mn_{0.021})_{3.000}(Al_{0.060}Fe^{3+}_{1.926}Cr_{0.002}Ti_{0.012})_{2.000}(Si_{3.015}Al_{0.000})_{3.015}$) in the rim, with small amounts of almandine (core), and spessartine (rim) components. Calcium content is uniform and stable in the core and rim, although the core contains small inclusions of epidote, quartz and rarely sphalerite. Andradite-rich zone (rim) displays increased Mn and Ti content in comparison with the grossular-rich phase (core) where these elements are below the detection limit (Table 1). The Fe component is significant in the rim approaching almost pure andradite (up to 96.9 %) with minor amounts of grossular, almandine and spessartine components.

REE and trace elements

The REE patterns of the studied skarn garnets are normalized to the chondrite value of McDonough & Sun (1995) and shown in Fig. 5. Y being a pseudolanthanide was included and plotted between Dy and Ho. Different zones during garnet growth display specific REE variations between different BSE coefficients in garnet grain. Fe-richer rim zone (BSE light zone, Fig. 4) exhibits LREE depletion (La, Ce, Pr and

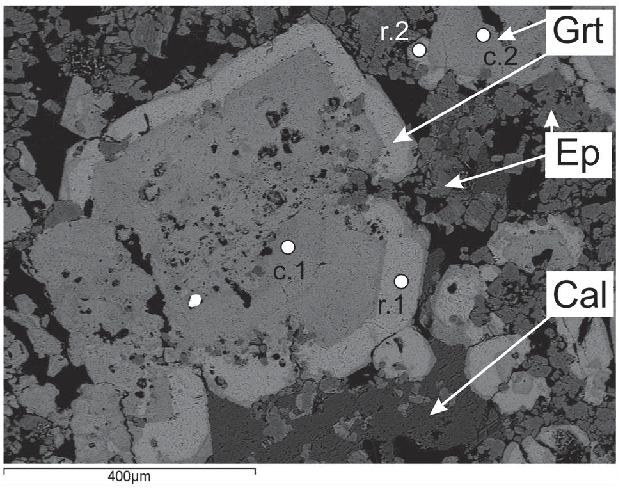

Fig. 4. BSE image of garnet grains with positions analyzed of EMPA and LA-ICP-MS methods.

Nd) and flat HREE pattern, with Sm maximum and Eu negative anomaly. On the other hand, Fe-poorer core zone (BSE dark zone, Fig. 4) shows a flat REE pattern without any significant enrichment or depletion. Studied garnet zones also show As, W, U, Th and Zr correlations. To be more specific, higher As and W enrichments (up to almost 12 times for both elements) strongly correlate with andradite-rich zone (rim), whereas U, Th, and Zr shows higher values (up to about 27 times for Th) in grossular-rich zone (core). The maximum value of U and Th is 3 ppm (Table 1).

Discussion

Analysing mineral zonation is a hard and challenging task due to the dimensions of the analysis pit to the relative scale of zonation and the angle of zonation margin to the imaged

Table 1: Representative LA-ICP-MS analyses of major elements in garnet SN-310 from studied skarns (in wt. % oxides (EMPA), rounded to second decimal place), structural formula, calculated end members (in mol. %) and measured trace elements (in ppm).

	SN-310			
	Grain 1		**Grain 2**	
	c. 1	**r. 1**	**c. 2**	**r. 2**
CaO	35.61	34.51	33.98	34.06
MnO	n.d.	0.26	n.d.	0.31
FeO	13.20	20.14	16.91	28.48
Al_2O_3	13.25	6.56	10.08	0.47
SiO_2	38.70	36.62	37.70	37.08
TiO_2	n.d.	0.67	n.d.	0.20
Cr_2O_3	n.d.	n.d.	0.01	0.03
Total	100.76	98.76	98.68	100.63
n.d. – not detected				
Garnet formula calculated on the basis of 12 oxygen atoms per formula unit (apfu)				
Si	2.991	2.962	3.012	3.015
Al	0.009	0.038	0.000	0.000
Sum	3.000	3.000	3.012	3.015
Al	1.198	0.588	0.961	0.060
Ti	0.000	0.041	0.000	0.012
Fe^{3+}	0.802	1.363	1.038	1.926
Cr	0.000	0.000	0.001	0.002
Sum	2.0009	1.992038	2.000	2.000
Fe^{2+}	0.051	0.000	0.091	0.011
Mn	0.000	0.018	0.000	0.021
Ca	2.949	2.991	2.909	2.968
Sum	3.000	3.009	3.00012	3.00028
End members				
Pyrope	0.0	0.0	0.0	0.0
Almandine	1.7	0.0	3.0	0.4
Spessartine	0.0	0.6	0.0	0.7
Grossular	58.2	28.9	45.0	1.9
Andradite	40.1	70.5	51.9	96.9
Uvarovite	0.0	0.0	0.0	0.1
Total	100.0	100.0	99.9	100.0
Trace elements (LA-ICP-MS)				
As	6.8±0.92	78.3±1.80	8.3±1.04	56.9±1.22
W	35.1±0.69	408±0.45	41.7±0.35	388±0.43
U	2.43±0.04	0.216±0.03	3.04±0.08	0.205±0.06
Th	3.01±0.05	0.110±0.05	2.72±0.02	0.178±0.06
Zr	119.8±1.37	13.2±1.33	117.2±1.30	11.8±0.62

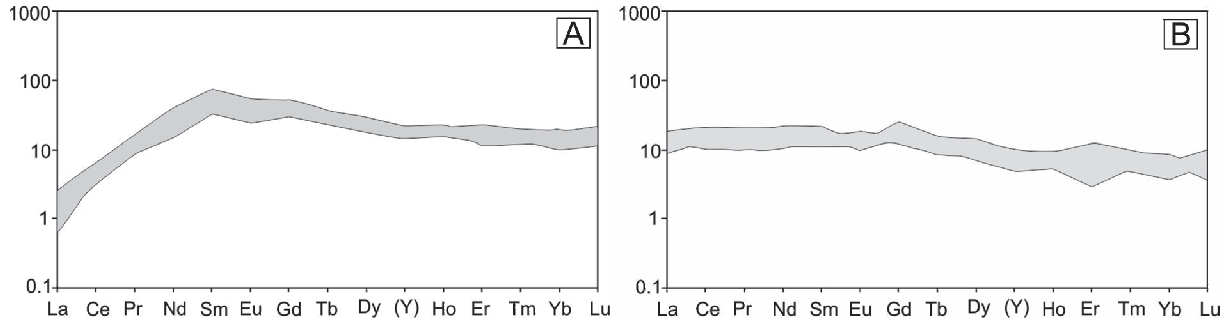

Fig. 5. REE pattern normalized to chondrite (McDonough & Sun 1995) of Fe-rich (**A**) vs. Fe-poor (**B**) zone.

surface (Smith et al. 2004). Fine zonation and heterogeneity could be resolved by choosing homogeneous domains within garnets and concentrating on large oscillatory zones, respectively.

The studied garnets have grown in a typical skarn rock, rich in ore minerals. Major and trace element zonal distributions reflect primarily the compositional heterogeneity of the protolith, changes in fluid composition during garnet growth, as well as, reactions controlled by fluid pathways. Zoned garnets with Al-rich cores and Fe-rich rims are the commonest in skarn systems, due to the tendency of early prograde garnets to be Al-enriched and retrograde in the first stage or later garnets to be Fe-enriched in the second stage (Einaudi et al. 1981; Nakano et al. 1991; Meinert 1992; Meinert et al. 1997). This phenomenon can be interpreted as a result of physicochemical changes in hydrothermal solutions during garnet growth.

Stowell et al. (1996) notice that first stage of garnet growth can be interpreted by diffusion in the local environment produced by metasomatism or change in temperature and pressure conditions. However, the small contact-metamorphic aureole, like that on Rudnik Mt. does not display any physical evidence for major variation and does not testify to large changes of pressure and temperature. In fact, garnet has kept growing since the initial first stage by infiltration of external hydrothermal fluids into the system. The pulse of magmatic-derived hydrothermal fluids has caused chemical overstepping of the previous garnet formed in equilibrium, leading to discontinuity in garnet composition.

The full process of partitioning major and trace elements between fluids and growing minerals involves removal of elements from the fluid, sorption onto a growing surface, incorporation via substitution mechanism, diffusion through the surface layer (McIntire 1963; Smith et al. 2004). Partitioning controlled by bulk crystal chemistry would be expected to occur during slow crystal growth, with the fluid chemistry buffered by the pre-existing local mineral/rock assemblage (Smith et al. 2004). Oscillatory zoning in garnets is interpreted as an early retrograde shock-induced feature related to high fluid pressure or as a result of externally induced local strain (e.g. Jamtveit et al. 1993; Ciobanu & Cook 2004). Further, according to Yardley et al. (1991), fluid flow through open systems produces oscillatory zoned garnets. Additionally, anisotropic garnets widely range in composition whereas the garnets near the end-member of andradite (Adr>90) are generally isotropic.

Trace elements such as Ti and Zr can provide information on petrological reactions and interpretations (Hickmott & Spear 1992). According to these authors, the higher Y can reflect reactions involving epidote, while elevated Ti can reflect reactions involving titanite (or ilmenite–rutile). Additionally, authors concluded that Y and Zr in garnet should follow Ca concentrations if the reaction for garnet growth involves epidote mineral consumption.

Thus, the sharp decrease of grossular component from core to rim in garnet SN-310 could reflect epidote consumption from the mineral assemblage. Stable Ca concentration values in Fe-rich and Fe-poor garnet zones involve another reaction where hydrothermal fluids were Fe carriers. The Fe content in skarn-forming fluids is closely related to their total salinity (Kwak et al. 1986).

Experimentally proven (Bau 1991), garnets in skarns which exhibit LREE depletion with negative or absent Eu anomaly, generally originate from the influence of neutral hydrothermal fluids. Following Gaspar et al. (2008) Al-rich garnets, which are anisotropic and twinned, form by prolonged interaction of pore fluids with the host rock, leading to a system buffered by the rock composition. They are commonly LREE depleted and HREE enriched, displaying weak positive or negative Eu anomalies. On the contrary, isotropic Fe-rich garnets that are LREE enriched and HREE depleted with strong positive Eu anomaly form by rapid growth from magmatic derived fluids.

The studied garnets from Rudnik coincide with the above described optical properties but their REE pattern is quite different. The Al-rich core displays flat REE pattern, whereas the Fe-rich rim is LREE depleted. Both zones display very weakly Eu negative anomaly. This could be a result of the Eu divalent state under reduced conditions which influences the behaviour of REEs (Gaspar et al. 2008). Prevailing of sulphide minerals, particularly pyrrhotite over magnetite at Rudnik (Stojanović et al. 2018) indicates reduced conditions where Eu should be present as Eu^{2+}.

Generally, hydrothermal fluids have a close relationship with boiling processes in the last phase of pluton

crystallization. According to Cvetković et al. (2016), the Rudnik ore field experienced magma mixing which accelerated the boiling process and provided conditions for strong hydrothermal activity. Boiling processes generally increase oxidation of remaining hydrothermal liquid. Oxidation rapidly increases the $\alpha_{Fe^{3+}}/\alpha_{Al^{3+}}$ ratio in the fluids and this corresponds to andradite precipitation on garnet rims (Jamtveit et al. 1993). As andradite concentration is almost pure in the rim, this can indicate the presence of a massive pulse of hydrothermal fluid, probably caused by the boiling process proposed formerly by Cvetković et al. (2016).

Further, Fe-rich garnets grow rapidly by advective metasomatism, at higher water/rock ratios (W/R), from magmatic-derived fluids, while Al-rich garnets are formed by diffusive metasomatism, at low W/R ratio, from host rock buffered metasomatic fluids (Gaspar et al. 2008). Significant presence of W suggests hydrothermal fluids derived from granitic pluton (Keppler & Wiyllie 1991). Such evidence has been recorded in a Fe-rich garnet zone and could indicate magmatic derived fluids responsible for andradite rim.

The magmatic origin of sulphur was already previously confirmed by the uniform values of isotope analyses obtained for various sulphide minerals in the Rudnik skarn deposit: δS34=+3.1±0.3 ‰ for sphalerite, +3.0 ‰ for pyrrhotite, and +3.3±0.6 ‰ for chalcopyrite (see Stojanović et al. 2018). Colloform bands composed of pyrite, pyrrhotite and siderite (Stojanović et al. 2018) can be attributed to hydrothermal pulse with magmatic origin interpretation.

Conclusion

In the polymetallic Pb–Zn Rudnik deposit, we conclude that:

- Rudnik skarns and hornfelses formed by contact-metamorphism of carbonate rocks, clastic rocks and shales during volcanic event that took place in the late Oligocene;
- The studied garnets from the Rudnik orefield show that in the first stage during garnet slow growth concentrations of REE were stable and probably buffered by mineral dissolution and reaction in the country rock. During the second stage and andradite-rich phase growth, which has been initiated by boiling process, the fluid composition was extremely controlled by the oxidation state, W/R ratio and salinity of solution;
- Garnets from Rudnik skarns widely range in composition whereas the garnets near the end-member of andradite (Adr>90) are generally isotropic.
- A large amount of sulphur minerals indicates reduced conditions and Eu divalent state that led to different behaviour of REEs;
- Hydrothermal fluids from the second stage could indicate magmatic origin of fluids, considering elevated W concentrations in the andradite garnet rim combined with sulphur isotopes in sulphide minerals;
- This study has not found either older or younger volcanic rocks than 23.9 Ma, in accordance with the results obtained by Cvetković et al. (2016).

Acknowledgments: This research was supported by project no. OI176019 of the Ministry of Education, Science and Technological Development of the Republic of Serbia. The authors thank the LA-ICP-MS laboratory, Geological Institute in Sofia, as well as the SEM laboratory, Faculty of Mining and Geology, University of Belgrade for support. The authors also wish to acknowledge the general support from all stuff of the Company Rudnik Mine.

References

Anđelković M. 1973: Geology of Mesozoic vicinity of Belgrade. *Annales Geologiques de la Peninsule Balkanique* 38, 1–136 (in Serbian).

Bau M. 1991: Rare-earth element mobility during hydrothermal and metamorphic fluid-rock interaction and the significance of the oxidation state of europium. *Chemical Geology* 93, 219–230. https://doi.org/10.1016/0009-2541(91)90115-8

Brković T. 1980: Explanatory booklet for sheet Kragujevac. In: Basic Geological Map of Yugoslavia 1:100,000. *Federal Geological Institute*, Belgrade, 1–82 (in Serbian with English and Russian summaries).

Brković T., Radovanović Z., Pavlović Z. & Dimitrijević M. 1980: Geological Map of Yugoslavia 1:100,000, Sheet Kragujevac. *Federal Geological Institute*, Belgrade.

Ciobanu L.C. & Cook I.N. 2004: Skarn textures and a case study: the Ocna de Fier-Dognecea orefield, Banat, Romania. *Ore Geology Reviews* 24, 315–370. https://doi.org/10.1016/j.oregeorev.2003.04.002

Cvetković V., Prelević D., Downes H., Jovanović M., Vaselli O. & Péskay Z. 2004: Origin and geodynamic significance of Tertiary postcollisional basaltic magmatism in Serbia (central Balkan Peninsula). *Lithos* 73, 161–186. https://doi.org/10.1016/j.lithos.2003.12.004

Cvetković V., Šarić K., Grubić A., Cvijić R. & Milošević A. 2014: The Upper Cretaceous ophiolite of North Kozara – remnants of an anomalous mid-ocean ridge segment of the Neotethys? *Geologica Carpathica* 65, 117–130. https://doi.org/10.2478/geoca-2014-0008

Cvetković V., Šarić K., Pecskay Z. & Gerdes A. 2016: The Rudnik Mts. Volcano-intrusive complex (central Serbia): An example of how magmatism controls metallogeny. *Geologia Croatica* 69, 89–99. https://doi.org/10.4154/GC.2016.08

Dimitrijević M.N. & Dimitrijević M.D. 1987: The Turbiditic Basins of Serbia. *Serbian Academy of Sciences and Arts Department of Natural & Mathematical Sciences*, Belgrade, 1–304.

Dimitrijević M.N. & Dimitrijević M.D. 2009: The Lower Cretaceous paraflysch of the Vardar zone: composition and fabric. *Annales Geologiques de la Peninsule Balkanique* 70, 9–21.

Einaudi M.T., Meinert L.D. & Newbery R.J. 1981: Skarn deposits. *Economic geology*, 75th Anniversary Volume, 317–391. https://doi.org/10.2113/gsecongeo.95.6.1183

Filipović I., Pavlović Z., Marković B., Rodin V., Marković O., Gagić N., Atin B. & Milićević M. 1978: Geological Map of Yugoslavia 1:100,000, Sheet Gornji Milanovac. *Federal Geological Institute*, Belgrade.

Gaspar M., Knaack C., Meinert D.L. & Moretti R. 2008: REE in skarn systems: A LA-ICP-MS study of garnets from the Crown

Jewel gold deposit. *Geochimica et Cosmochimica Acta* 72, 185–205. https://doi.org/10.1016/j.gca.2007.09.033

Haas J. & Péró C. 2004: Mesozoic evolution of the Tisza Megaunit. *International Journal of Earth Sciences* 93, 297–313. https://doi.org/10.1007/s00531-004-0384-9

Hickmott D.D. & Spear F.S. 1992: Major and trace-element zoninig in metamorphic garnets from calcareous pelites in the NW Shelburne Falls quadrangle, Massachusetts: garnet growth histories in retrograded rocks. *Journal of Petrology* 33, 965–1005. https://doi.org/10.1093/petrology/33.5.965

Horvath F., Bada G., Szafian P., Tari G., Adam A. & Cloetingh S. 2006: Formation and deformation of the Pannonian Basin: Constraints from observational data. In: Gee D.G. & Stephenson R.A. (Eds.): European Lithosphere Dynamics. *Geological Society, London, Memoirs* 32, 191–206.

Jackson S.E., Pearson N.J., Griffin W.L. & Belousova E.A. 2004: The application of laser ablation-inductively coupled plasma-mass spectrometry to in situ U-Pb zircon geochronology. *Chemical Geology* 211, 47–69. https://doi.org/10.1016/j.chemgeo.2004.06.017

Jamtveit B. & Hervig R.L. 1994: Constraints on Transport and Kinetics in Hydrothermal Systems from Zoned Garnet Crystals. *Science* 263, 505–508. https://doi.org/10.1126/science.263.5146.505

Jamtveit B., Wogelius R. & Fraser D. 1993: Zonation patterns of skarn garnets: Records of hydrothermal system evolution. *Geology* 21, 113–116. https://doi.org/10.1130/0091-7613(1993)021<0113:ZPOSGR>2.3.CO;2

Jamtveit B., Ragnarsdottir K.V. & Wood B.J. 1995: On the origin of zoned grossular-andradite garnets in hydrothermal systems. *European Journal of Mineralogy* 7, 1399–1410. https://doi.org/10.1127/ejm/7/6/1399

Keppler H. & Wiyllie P.J. 1991: Partitioning of Cu, Sn, Mo, W, U and Th between melt and aqueous fluid in the systems haplogranite-H_2O-HCl and haplogranite-H_2O-HF. *Contributions to Mineralogy and Petrology* 109, 139–150. https://doi.org/10.1007/BF00306474

Kwak P.T., Brown M.W., Abeysinghe B.P. & Tan H.T. 1986: Fe Solubilities in very saline hydrothermal fluids: Their relation to zoning in some ore deposits. *Economic Geology* 81, 447–465. https://doi.org/10.2113/gsecongeo.81.2.447

Ludwig K.R. 2013: User's manual for Isoplot 3.75. A Geochronological Toolkit for Microsoft Excel. *Berkeley Geochronology Center, Special Publication* 5, 1–75. http://www.bgc.org/isoplot_etc/isoplot.html

McDonough W.F. & Sun S. 1995: The composition of the Earth. *Chemical Geology* 120, 223–253. https://doi.org/10.1016/0009-2541(94)00140-4

McIntire W.L. 1963: Trace element partition coefficients – a review of theory and application to geology. *Geochimica et Cosmochimica Acta* 27, 1209–1264. https://doi.org/10.1016/0016-7037(63)90049-8

Meinert D.L. 1992: Skarns and skarn deposits. *Geoscience Canada* 19, 145–162. https://doi.org/10.12789/gs.v19i4.3773

Meinert D.L., Hefton K.K., Mayes D. & Tasiran I. 1997: Geology, zonation, and fluid evolution of the Big Gossan Cu–Au skarn deposit, Irian Jaya. *Economic Geology* 92, 509–534. https://doi.org/10.2113/gsecongeo.92.5.509

Mladenović D., Batoćanin N., Vulić P. & Srećković-Batoćanin D. 2018: Rare earth elements in garnets in the skarn from the Rogozna Mts. *Proceedings of the XVII Serbian Geological Congress, Vrnjačka Banja*, vol. I, 60–62 (in Serbian).

Nakano T., Yoshino T., Shimazaki H. & Shimizu M. 1991: Pyroxene composition as an indicator in the classification of skarn deposits. *Economic Geology* 89, 1567–1580. https://doi.org/10.2113/gsecongeo.89.7.1567

Nicolescu S., Cornell D., Sodervall U. & Odelius H. 1998: Secondary ion mass spectrometry analysis of rare earth elements in grandite garnet and other skarn related silicates. *European Journal of Mineralogy* 10, 251–259. https://doi.org/10.1127/ejm/10/2/0251

Pamić J. & Šparica M. 1983: The age of the volcanic of Požeška Gora (Croatia, Yugoslavia). *Radovi Jugoslovenske Akademije Znanosti i Umjetnosti* 404, 183–198.

Park C., Song Y., Kang I., Shim J., Chung D. & Park C. 2017: Metasomatic changes during periodic fluid flux recorded in grandite garnet from the Weondong W-skarn deposit, South Korea. *Chemical Geology* 451, 135–153. https://doi.org/10.1016/j.chemgeo.2017.01.011

Paton C., Hellstrom J., Paul B., Woodhead J. & Hergt J. 2011: Iolite: Freeware for the visualization and processing of mass spectrometric data. *Journal of Analytical Atomic Spectrometry* 26, 2508–2512. https://doi.org/10.1039/c1ja10172b

Pollok K., Jamtveit B. & Putnis A. 2001: Analytical transmission electron microscopy of osscillatory zoned grandite garnets. *Contributions to Mineralogy and Petrology* 141, 358–366. https://doi.org/10.1007/s004100100248

Prelević D., Foley S.F., Romer L., Cvetković V. & Downes H. 2005: Tertiary Ultrapotassic Volcanism in Serbia: Constraints on Petrogenesis and Mantle Source Characteristics. *Journal of Petrology* 46, 1443–1487. https://doi.org/10.1093/petrology/egi022

Prelević D., Wehrheim S., Reutter M., Romer R., Boev B., Božović M., Bogaard P., Cvetković V. & Schmid S. 2017: The Late Cretaceous Klepa basalts in Macedonia (FYROM) – Constrains on the final stage of Tethys closure in the Balkans. *Terra Nova* 23, 145–153. https://doi.org/10.1111/ter.12264

Schmid M., Bernoulli D., Fugenschuh B., Matenco L., Schefer S., Schuster R., Tischler M. & Ustaszewski K. 2008: The Alpine–Carpathian–Dinaridic orogenic system: correlation and evolution of tectonic units. *Swiss Journal of Geoscience* 101, 139–183. https://doi.org/10.1007/s00015-008-1247-3

Sladić-Trifunović M., Pantić N. & Mihajlović Đ. 1989: The significance of clastic limestone in the section of Bela Reka – Resnik, for stratigraphic interpretation and reconstruction of the depositional environments of the Upper Jurassic–Lower Cretaceous deep-complexes in the vicinity of Belgrade. In: *Proceedings SGD* for 1987, 1988 and 1989.

Smith M., Henderson P., Jeffries T., Long J. & Williams C. 2004: The rare earth elements and uranium in garnets from the Beinn an Dubhaich aureole, Skye, Scotland, UK: Constraints on processes in a dynamic hydrothermal system. *Journal of Petrology* 45, 457–484. https://doi.org/10.1093/petrology/egg087

Somarin A.K. 2004: Garnet composition as an indicator of Cu mineralization: Evidence from skarn deposit of NW Iran. *Journal of Geochemical Exploration* 81, 47–57. https://doi.org/10.1016/S0375-6742(03)00212-7

Srećković-Batoćanin D., Vasković N., Milutinović S., Ilić V. & Nikić Z. 2014: Composition of zonal garnets from the garnetite exoskarn of the ore field Rogozna (Rogozna Mts, southern Serbia). *Proceedings of the XVI Serbian Geological Congress, Donji Milanovac*, 265–269.

Stojanović J., Radosavljević S., Tošović R., Pačevski A., Radosavljević-Mihajlović A., Kašić V. & Vuković N. 2018: A review of the Pb-Zn-Cu-Ag-Bi-W polymetallic ore from the Rudnik orefield, Central Serbia. *Annales Geologiques de la Peninsule Balkanique* 79, 47–69.

Stowell H., Menard T. & Ridgway C. 1996: Ca-Metasomatism and chemical zonation of garnet in contact-metamorphic aureoles, Juneau gold belt, southeastern Alaska. *The Canadian Mineralogist* 34, 1195–1209.

Tančić P., Vulić P., Kaindl R., Sartory B. & Dimitrijević R. 2012: Macroscopically-zoned grandite from the garnetite skarn of

Meka Presedla (Kopaonik Mountain, Serbia). *Acta Geologica Sinica* 86, 393–406.

Tančić P., Kremenović A. & Vulić P. 2020: Structural dissymmetrization of optically anisotropic $Grs_{64\pm1}Adr_{36\pm1}Sps_2$ grandite from Meka Presedla (Kopaonik Mt., Serbia). *Powder Diffraction* 35, 7–16. https://doi.org/10.1017/S0885715619000897

Ustaszewski K., Kounov A., Schmid S., Schaltegger U., Krenn E., Frank W. & Fügenschuh B. 2010: Evolution of the Adria-Europe plate boundary in the northern Dinarides: From continent-continent collision to back-arc extension. *Tectonics* 29, 1–34. https://doi.org/10.1029/2010TC002668

Wiedenbeck M.P., Corfu A.F., Griffin W.L., Meier M., Oberli F., von Quadt A., Roddick J.C. & Spiegel W. 1995: Three natural zircon standards for U–Th–Pb, Lu–Hf, trace element and REE analyses. *Geostandards and Geoanalytical Research* 19, 1–23. https://doi.org/10.1111/j.1751-908X.1995.tb00147.x

Xiao X., Zhou T., White N., Zhang L., Fan Y., Wang F. & Chen X. 2018: The formation and trace elements of garnet in the skarn zone from the Xinqiao Cu-S-Fe-Au deposit, Tongling ore district, Anhui Province, Eastern China. *Lithos* 302–303, 467–479. https://doi.org/10.1016/j.lithos.2018.01.023

Yardley D.W.B., Rochelle A.C., Barnicoat C.A. & Lloyd E.G. 1991: Oscillatory zoning in metamorphic minerals: an indicator of infiltration metasomatism. *Mineralogical Magazine* 55, 357–365. https://doi.org/10.1180/MINMAG.1991.055.380.06

Zhai D., Liu J., Zhang H., Wang J., Su L., Yang X. & Wu S. 2014: Origin of oscillatory zoned garnets from the Xieertala Fe–Zn skarn deposit, northern China: In situ LA–ICP-MS evidence. *Lithos* 190–191, 279–291. https://doi.org/10.1016/j.lithos.2013.12.017